Chemosphere 363 (2024) 142880

Contents lists available at ScienceDirect

Chemosphere

journal homepage: www.elsevier.com/locate/chemosphere

Chemical composition of PM_{10} at a rural site in the western Mediterranean and its relationship with the oxidative potential

Noelia Gómez-Sánchez, Nuria Galindo *, Marina Alfosea-Simón, Jose F. Nicolás, Javier Crespo, Eduardo Yubero

Atmospheric Pollution Laboratory (LCA), Department of Applied Physics, Miguel Hernández University, Avenida de la Universidad S/N, 03202, Elche, Spain

HIGHLIGHTS

- PM_{10} mainly made up of organic matter and crustal components.
- WSOC and MSOC come from combustion sources and secondary aerosol formation.
- OP^{AA} was not strongly correlated with any of the species measured.
- Moderate to strong correlations between OP^{DTT} and biomass burning tracers.
- PM_{10} is not a good metric for aerosol toxicity in the study area.

GRAPHICAL ABSTRACT

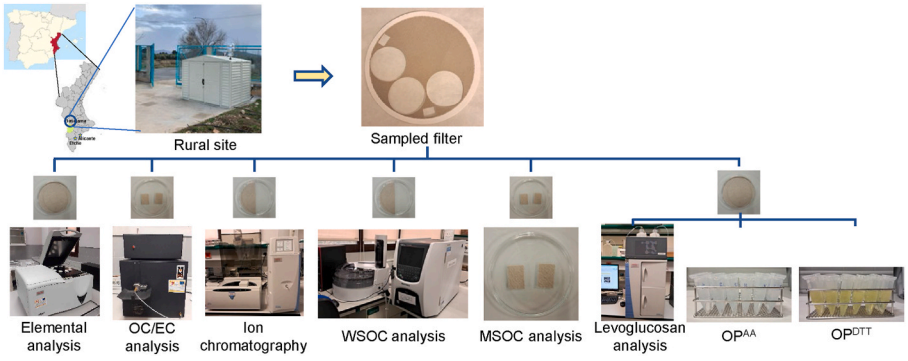

ARTICLE INFO

Handling editor: R Ebinghaus

Keywords:
PM_{10} composition
Oxidative potential
Dithiothreitol
Ascorbic acid
Rural location

ABSTRACT

A comprehensive chemical characterization (water-soluble ions, organic and elemental carbon, water- and methanol-soluble organic carbon, levoglucosan, and major and trace metals) of PM_{10} samples collected in a rural area located in the southeast of the Iberian Peninsula was performed. Additionally, the oxidative potential of the samples, used as an indicator of aerosol toxicity, was determined by the ascorbic acid (OP^{AA}) and dithiothreitol (OP^{DTT}) assays. The average concentration of PM_{10} during the study period, spanning from late winter to early spring, was 20.2 ± 10.8 μg m^{-3}. Nitrate, carbonate and calcium (accounting for 20% of the average PM_{10} mass concentration) and organic matter (with a contribution of 28%) were the main chemical components of PM_{10}. Average concentrations of traffic tracers such as elemental carbon, copper and zinc (0.31 μg m^{-3}, 3 ng m^{-3}, and 9 ng m^{-3}, respectively) were low compared with those obtained at an urban site in the same region, due to the almost total absence of traffic in the surrounding of the sampling site. Regarding levoglucosan and K^+, which can be considered as tracers of biomass burning, their concentrations (0.12 μg m^{-3} and 55 ng m^{-3}, respectively) were in the lower range of values reported for other rural areas in Europe, suggesting a moderate contribution form this source to PM_{10} levels. The results of the Pearson's correlation analysis showed that volume-normalised OP^{AA} and OP^{DTT} levels (average values of 0.11 and 0.32 nmol min^{-1} m^{-3}, respectively) were sensitive to different PM_{10} chemical components. Whereas OP^{AA} was not strongly correlated with any of the species measured, good

* Corresponding author.
E-mail addresses: noelia.gomezs@umh.es (N. Gómez-Sánchez), ngalindo@umh.es (N. Galindo), malfosea@umh.es (M. Alfosea-Simón), j.nicolas@umh.es (J.F. Nicolás), jcrespo@umh.es (J. Crespo), eyubero@umh.es (E. Yubero).

https://doi.org/10.1016/j.chemosphere.2024.142880
Received 27 March 2024; Received in revised form 10 July 2024; Accepted 15 July 2024
Available online 15 July 2024

correlation coefficients of OP^{DTT} with water-soluble organic carbon (r = 0.81) and K^+ (r = 0.73) were obtained, which points to biomass burning as an important driver of the DTT activity.

1. Introduction

Air pollution has been recognised as one of the main causes of premature deaths in the world. Particulate matter (PM) is the pollutant of greatest concern since it was responsible for almost 240000 premature deaths in Europe in 2020, far ahead of nitrogen dioxide and ozone (EEA, 2022). Exposure to PM has been linked to cardiovascular and respiratory diseases (Newell et al., 2017), cancer (Turner et al., 2020), adverse pregnancy outcomes (Hannam et al., 2014), psychiatric disorders (Borroni et al., 2022) and cognitive decline (Kilian and Kitazawa, 2018).

Recent research indicates that the adverse effects of atmospheric PM on human health at the cellular level are linked to the production of oxidative stress (Chirino et al., 2010; Lionetto et al., 2021; Pietrogrande et al., 2019). This occurs when the generation of oxidising agents exceeds the available antioxidant defences. The primary oxidising agents are reactive oxygen species (ROS). These species are oxygen-containing molecules, such as hydroxyl radical (HO·) and superoxide anion ($O_2^{\cdot-}$), that have one or more unpaired electrons, which make them highly reactive. ROS are normal products of aerobic cell metabolism; however, the enhanced ROS production can induce molecular damage since they readily react with proteins, lipids and nucleic acids (Grahame and Schlesinger, 2012). The ability of PM to produce oxidative stress is called oxidative potential (OP) and is recognised as a better exposure metric than just PM mass concentrations (Calas et al., 2018).

Different acellular assays, which are faster and less resource intensive than cellular assays, have been recently developed to measure the OP of atmospheric aerosol samples (Bates et al., 2019; Pietrogrande et al., 2019). Among these methods, the dithiothreitol (DTT) and ascorbic acid (AA) assays are probably the most used because they are simple, fast and inexpensive. These methods are based on the measurement of the depletion rate of DTT and AA, which can be considered a proxy for cellular reductants and antioxidants, respectively. The responses of both methods to different PM components and, in turn, to different PM sources may vary depending on the assay, the characteristics of the sampling site and the season of the year (Bates et al., 2019; Calas et al., 2019; Clemente et al., 2023a; Patel and Rastogi, 2018).

The study of the concentrations, chemical composition and OP levels of atmospheric aerosols at rural sites provides information on the background conditions in a given geographic area. So far, studies on the relationship between PM chemical composition and the OP in rural areas, far from anthropogenic sources, are still scarce. In the present work, a comprehensive chemical characterization of PM_{10} samples collected at a rural site in southeastern Spain was performed, including different carbonaceous components such as elemental carbon (EC), total organic carbon (OC), water-soluble organic carbon (WSOC), methanol-soluble organic carbon (MSOC) and levoglucosan, considered a specific tracer of biomass burning (Bhattarai et al., 2019). The OP of the samples using the DTT and AA assays was also determined and the relationship between chemical components and OP measurements was analysed. OP values measured in the present study were compared with those previously obtained at an urban site in the same region (Clemente et al., 2023a) with the aim of evaluating the sensitivity of both assays to the site typology and contribute to our knowledge on the use of OP as a predictor of aerosol toxicity, which is still a matter of debate (Dominutti et al., 2023; Pietrogrande et al., 2022).

2. Materials and methods

2.1. Sampling site and PM_{10} measurements

PM samples were collected in Benejama, a small town (~1700 inhabitants) located in the northwest of the province of Alicante (southeastern Iberian Peninsula, Fig. 1), approximately 45 km from the Mediterranean coast. The town is located in a flat valley (~600 m above sea level) surrounded by crop lands (mainly, olive trees and vineyards).

Benejama has a Mediterranean climate. Summers are short and hot, with a maximum daily average temperature of around 27 °C, while winters are long and cold. During this season average daily minimum and maximum temperatures oscillate between 4 and 16 °C. The sampler was located in a school yard on the outskirts of the town, far from significant PM emission sources.

Twenty-four-hour PM_{10} samples were collected daily between 22 February and 4 April 2023 by means of a MCV high-volume sampler (30 $m^3\ h^{-1}$). A total of thirty-eight samples were collected onto 150-mm quartz fibre filters (MK 360, Ahlstrom) during the measurement campaign. Mass concentrations were determined gravimetrically using a Mettler-Toledo model XP105 analytical balance with 10 μg sensitivity. Filters were kept in controlled conditions (20 ± 1 °C and 50 ± 5% relative humidity) for at least 24-h and weighted in quadruplicate before and after sampling. Samples were stored in the fridge at 4 °C until chemical analyses.

The campaign also included the measurement of meteorological variables by means of a Davis Vantage Pro2 weather station located approximately 350 m from the sampling site.

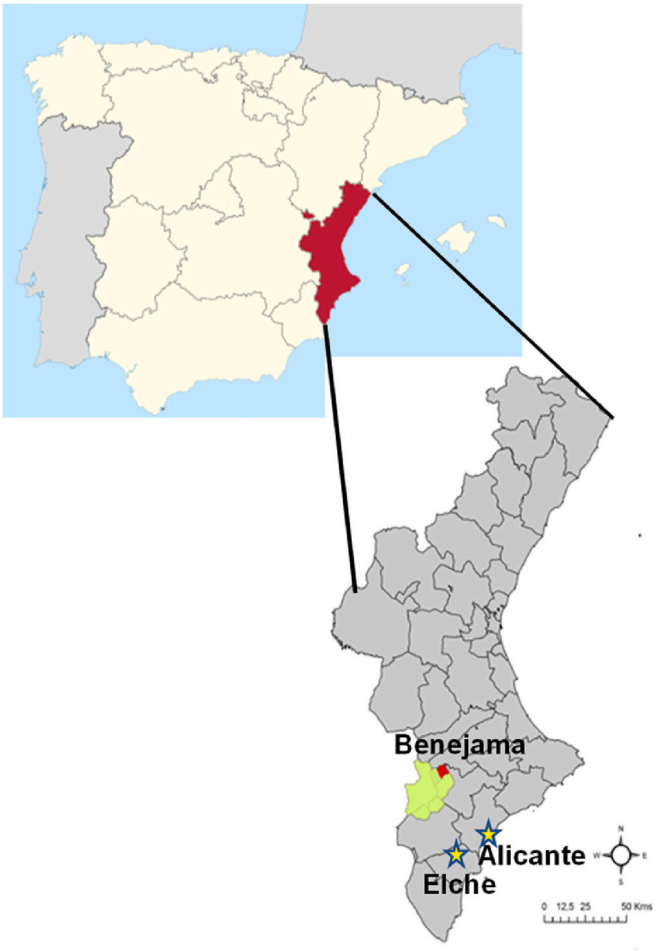

Fig. 1. Location of the sampling site in southeastern Spain.

2.2. Chemical analyses

Elemental analysis was performed on a 47-mm diameter filter punch by means of Energy Dispersive X-Ray Fluorescence (ED-XRF). An ARL Quant'x Spectrometer (Thermo Fisher Scientific, UK) with a Si(Li) detector was used. Details of the analytical setup are given in Chiari et al. (2018).

EC and OC were determined using a Thermal-Optical Carbon Aerosol Analyser (Sunset Laboratory, Inc.). All samples were analysed in duplicate. For this, two filter punches (1.5 cm^2 each) were analysed separately with the EUSAAR2 temperature protocol, and EC and OC concentrations were calculated as the average value of the two measurements. To estimate MSOC concentrations, a 1.5 cm^2 filter punch was immersed in 1 mL of methanol for 2 h. The punch was dried in air for 24 h, and analysed for OC and EC using the thermal-optical method (Cheng et al., 2016). These measurements were also carried out in duplicate. MSOC concentrations were calculated by subtracting the OC mass concentration after methanol extraction from the total OC concentration. MSOC is often considered as a proxy for brown carbon, i.e. light absorbing organic carbon (Cao et al., 2021; Cheng et al., 2016), and has been identified to have a stronger OP than WSOC in some previous works (Cao et al., 2021).

An 8.7 cm^2 filter punch of each PM_{10} sample was extracted in 6.5 mL of deionized water under sonication for 45 min. The extracts were filtered using nylon 0.45-μm pore syringe filters and analysed by ion chromatography to determine water-soluble ion concentrations. The analysis of cations was performed on a Dionex ICS-1100 ion chromatograph with a CS12A column (4 × 250 mm) using methane sulfonic acid as eluent (20 mM, 0.8 mL min^{-1}). Anions were determined on a Dionex Aquion system (Thermo Fisher Scientific) equipped with an AS11-HC analytical column (4 × 250 mm) and NaOH as eluent (15 mM, 1 mL min^{-1}).

A TOC-L CSH analyser (Shimadzu) was used to determine WSOC and inorganic carbon concentrations. Punches (8.7 cm^2) of each PM_{10} filter were extracted in 7.5 mL of deionized water, sonicated for 45 min and filtered through nylon 0.45-μm pore syringe filters. A platinum catalyst at 680 °C was used to convert the carbon in filtered extracts into CO_2, which was measured by a nondispersive infrared detector (NDIR). WSOC was quantified as the non-purgeable organic carbon. For this, water extracts were acidified with 1 M HCl and purged with pure air in order to remove dissolved inorganic carbon and volatile organics. Inorganic carbon (IC) was then estimated from the difference between the total carbon and the WSOC.

Finally, a 47-mm diameter filter punch was extracted in 12 mL of water by ultrasonic agitation during 45 min and analysed to determine the levoglucosan content and OP of PM_{10} samples, after filtration to remove insoluble particles and any filter fibre. Levoglucosan was quantified by high-performance anion exchange chromatography with pulsed amperometric detection (HPAEC-PAD) using a Thermo Scientific Dionex Integrion system equipped with a two-way valve. This setting allows to alternately run two NaOH solutions with different concentrations. The separation was carried out on a Dionex Carbopac PA1 column (250 × 4 mm) with 30 mM NaOH eluent at a flow rate of 0.5 ml min^{-1}. After 25 min run time, the column was cleaned with 200 mM NaOH for 8 min and re-equilibrated with 25 mM NaOH for 17 min before the injection of the next sample. For the amperometric detection a gold working electrode was used.

2.3. OP measurements and correlation analysis

OP analyses were performed on PM_{10} water extracts using the AA and DTT assays (Clemente et al., 2023a). Equivalent PM_{10} concentrations in the extracts generally ranged from 60 to 200 μg mL^{-1}. In the AA assay, 1.5 mL of the PM_{10} extracts were incubated at 37 °C with 1.35 mL of 0.1 M potassium phosphate buffer (pH = 7.4) for 10 min. Then, 150 μL of 2 mM AA were added to the solution. At different reaction times (usually 15, 30 and 45 min to ensure a linear kinetic behaviour), the remaining AA was determined spectrophotometrically at 265 nm.

For the DTT assay, three aliquots of 0.45 mL of the sample extracts were incubated at 37 °C with 90 μL of 0.1 M potassium phosphate buffer (pH = 7.4) for about 5 min, after which 60 μL of 1 mM DTT were added. Subsequently, 0.5 mL of trichloroacetic acid (10% w/v) were added to each aliquot at 15, 25 and 35 min to ensure a linear kinetic behaviour. Finally, 2 mL of Tris-EDTA (0.4 M Tris with 20 mM EDTA) and 50 μL of 10 mM 5,5′-dithiobis-2-nitrobenzoic acid (DTNB) were added to the mixture and the absorbance of the solution was measured at 412 nm.

The initial concentration of AA and DTT in the solutions was 100 nmol mL^{-1}. Blank filters were analysed following the same procedures as those of PM_{10} samples. All assays were run in duplicate.

Volume-normalised AA and DTT activities (OP_v) in nmol min^{-1} m^{-3} were calculated as follows.

$$OP_V = \frac{-\left(a_{sample} - a_{bl}\right) \cdot V_{ext} \cdot A_{filter}}{V_a \cdot V_{air} \cdot A_{punch}}$$

where a_{sample} and a_{bl} are the depletion rates of AA or DTT (in nmol min^{-1}) in the sample and blank extracts, respectively; V_{ext} is the extraction volume (12 mL); V_a is the volume of sample used in the assay (1.5 mL for the AA assay and 0.45 mL for the DTT assay); V_{air} is the sampled air volume (in m^3); and A_{filter} and A_{punch} (cm^2) are the total areas of the filter and the filter punches used for analysis.

Mass-normalised OP values (OP_m, nmol min^{-1} μg^{-1}), referred as intrinsic oxidative potential, were subsequently obtained by dividing OP_v by the atmospheric concentration of PM_{10}.

To assess whether there are statistically significant relationships between OP values and PM_{10} chemical components, and also among other analysed parameters, the Pearson's correlation coefficients were applied.

3. Results and discussion

3.1. PM_{10} concentrations

The average PM_{10} concentration during the measurement period was 20.2 ± 10.8 μg m^{-3}. Daily mean levels varied between 8.5 and 73.6 μg m^{-3} (Fig. 2). Maximum concentrations were measured at the beginning of the sampling period and were due to an intense Saharan dust event affecting the study area. When these two values were removed from the data base, the average PM_{10} concentration was 10% lower and much less variable (18.2 ± 5.1 μg m^{-3}).

PM_{10} levels observed in this study are of the same order of those registered at other background sites in the Mediterranean region such as the Capo Granitola Observatory (Sicily, 23.2 μg m^{-3}; Dinoi et al., 2017) or the Għarb rural background station (Maltese archipelago, 18.2 μg m^{-3}; Scerri et al., 2016). However, these values are low compared with those measured at rural sites heavily impacted by anthropogenic sources

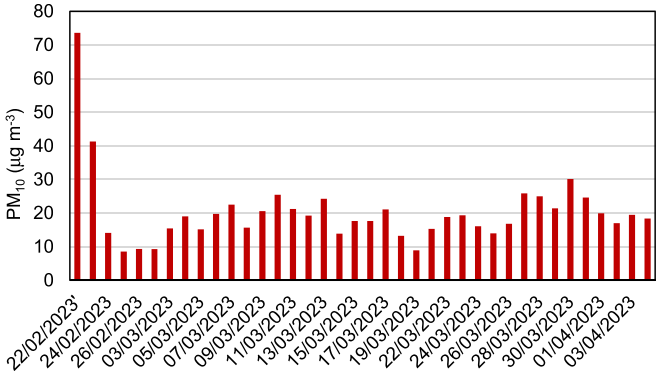

Fig. 2. Daily PM_{10} concentrations between late February and early April 2023.

such as biomass burning (>30 μg m^{-3}; Pérez-Pastor et al., 2020; Pietrogrande et al., 2021).

When concentrations at the rural site are compared with those recorded at other locations within the same geographical area, it can be observed that the average PM_{10} value measured in this study is between the levels reported for a regional background station (~14 μg m^{-3}; Clemente et al., 2023b; Galindo et al., 2017) and those observed at residential (25 μg m^{-3}; Galindo et al., 2021) and urban sites in Elche (~30 μg m^{-3}; Clemente et al., 2023b) located close to the Mediterranean coast, approximately 50 km from the monitoring site (Fig. 1).

3.2. Ionic components

Average concentrations of the water-soluble ions measured in PM_{10} samples are presented in Table 1. The mean carbonate concentration, estimated from inorganic carbon concentrations obtained with the TOC analyser, is also shown. It is worth mentioning that a strong correlation ($r = 0.95$, $p < 0.05$) between IC concentrations and the anion deficit, calculated from the ionic balance between cations and anions (Nicolás et al., 2009), was obtained. Additionally, the correlation coefficient between IC and Ca^{2+} concentrations (excluding the two highest PM_{10} values) was good ($r = 0.86$, $p < 0.05$). These results indicate that the anion deficit can be mainly attributed to calcium carbonate and bicarbonate.

Nitrate, carbonate and calcium were the most abundant ions, representing around 20% of the total PM_{10} mass concentration. The mean calcium concentration was similar to that found in a residential area within the same study region (Galindo et al., 2021) and significantly higher than the values found at other rural sites in southern Europe (<0.4 μg m^{-3}; Malaguti et al., 2015; Pietrogrande et al., 2021). Similarly, the average IC concentration found in the present study (0.41 μg m^{-3}) was higher than the value found at a rural site in Southern Italy (0.17 μg m^{-3}; Malaguti et al., 2015). The most likely reason is that soils in our study area are enriched with calcium carbonate.

Sulfate, nitrate and oxalate showed good correlations among them ($r > 0.73$, $p < 0.05$), pointing to a common origin from atmospheric photochemical reactions of gaseous precursors. This was not unexpected since a substantial fraction of oxalic acid (the most abundant organic dicarboxylic acid) is thought to be of secondary origin. Significant associations between oxalate and secondary inorganic ions, particularly sulfate, have been found in a number of previous studies (Laongsri and Harrison, 2013; Navarro-Selma et al., 2022; Jiang et al., 2014; Zhou et al., 2015). In contrast, no correlation between secondary ions and carbonate was found, since CO_3^{2-} mainly comes from soil dust. In fact, carbonate concentrations were positively correlated with temperature ($r = 0.63$, $p < 0.05$) and negatively correlated with relative humidity ($r = -0.58$, $p < 0.05$), most likely because resuspension of soil dust is favoured by high ambient temperatures and low relative humidity.

Magnesium and chloride were highly correlated with sodium ($r > 0.9$, $p < 0.05$), as already observed in the study area (Galindo and Yubero, 2017). The slope of the regression line between Mg^{2+} and Na^+ (0.13) was very close to the mass ratio between these two ions in seawater (0.12; Millero et al., 2008). However, the linear regression between Cl^- and Na^+ showed a slope of 1.44, slightly lower than the Cl^-/Na^+ mass ratio found in seawater (1.8; Millero et al., 2008). This indicates a deficit of Cl^- caused by the reactions of acids with NaCl during the transport of marine aerosols from the coast, which results in the loss of chloride as HCl gas.

K^+ concentrations were low compared with those measured at other sites in the Mediterranean basin (Malaguti et al., 2015; Pietrogrande et al., 2021), including the residential location mentioned above (0.26 μg m^{-3}; Galindo et al., 2021). Soluble potassium can be emitted by multiple sources such as biomass burning, soil dust, sea salt, cooking, industry and fertilizers (Pachon et al., 2013; Urban et al., 2012). In the present study, K^+ did not show any correlation with Na^+ and Ca^{2+}, indicating that sea salt and soil dust did not significantly contribute to potassium emissions during the study period. In contrast, the correlation with levoglucosan was moderately good ($r = 0.67$, $p < 0.05$), which points to biomass burning as the main source of potassium during the measurement campaign. Therefore, the low K^+ concentrations may indicate that the sampling site was moderately influenced by wood burning emissions during the study period.

3.3. Carbonaceous species

3.3.1. Organic and elemental carbon

Table 2 shows mean concentrations of the carbonaceous components analysed in the samples. EC levels were low, as expected for a rural site with little influence of direct exhaust emissions. The average EC concentration was very similar to those reported for other Mediterranean rural sites (Dinoi et al., 2017; Malaguti et al., 2015) and much lower than the values found at urban stations (Clemente et al., 2023b; Dinoi et al., 2017). The mean OC concentration was approximately half the observed levels in residential and urban areas located in the same study region (Galindo et al., 2021; Clemente et al., 2023b), as a result of lower emissions from traffic and other anthropogenic sources. These emissions include the release of primary OC and gaseous precursors of secondary organic aerosols. Similar outcomes have been described in previous studies (Dinoi et al., 2017; Laongsri and Harrison, 2013). Organic matter (OM), calculated by multiplying OC by a factor of 1.8 recommended for rural sites (Chow et al., 2015), accounted for 28% of the average PM_{10} mass concentration. This contribution was lower than that found at other rural sites in Europe (Błaszczak and Mathews, 2020; Borlaza et al., 2022), most likely because of higher dust loads favoured by the low vegetative cover of the study region and also due to lower OM emissions from biomass burning and biogenic sources.

3.3.2. Water-soluble organic carbon

WSOC concentrations (Table 2) are in line with measurements made at other rural sites in Europe (Laongsri and Harrison, 2013; Sandrini et al., 2016), although the results are not fully comparable since the sampling campaigns were carried out in different seasons or had a different duration. However, the value of 1.33 μg m^{-3} found in the present study was slightly higher than the annual mean concentration registered for PM_1 at an urban background site in Elche (0.95 μg m^{-3}; López-Caravaca et al., 2023). Although previous works have reported

Table 1
Mean concentrations and standard deviations (SD) of water-soluble species (μg m^{-3}).

Ion	Mean	SD
Cl^-	0.47	0.44
NO_3^-	1.36	0.86
SO_4^{2-}	0.83	0.45
CO_3^{2-}	2.07	0.77
$C_2O_4^{2-}$	0.09	0.04
Na^+	0.38	0.29
NH_4^+	0.29	0.17
K^+	0.12	0.06
Mg^{2+}	0.08	0.04
Ca^{2+}	1.03	0.37

Table 2
Mean concentrations and standard deviations (SD) of carbonaceous species. All concentrations are given in μg m^{-3}, except for levoglucosan (ng m^{-3}).

Component	Mean	SD
EC	0.31	0.12
OC	3.11	0.47
MSOC	1.96	0.31
WSOC	1.33	0.32
Levoglucosan	55	29

higher WSOC levels at urban sites than at rural stations (Li et al., 2023; Sandrini et al., 2016), it has to be considered that different PM size fractions were measured at the rural and urban background locations. In addition, traffic restrictions due to COVID-19 were still in place at the urban background site during the measurement period.

The WSOC/OC ratio found in the present study was 0.42, implying that 42% of OC is water-soluble. This value was in the lower range of those reported for rural sites worldwide (0.45–0.61; Pio et al., 2007; Ram and Sarin, 2010; Suto and Kawashima, 2021; Szidat et al., 2009; Theodosi et al., 2018; Xie et al., 2019). WSOC is generally formed by oxygenated organic compounds and includes different classes of polar species such as carboxylic acids and sugar compounds (e.g. levoglucosan). It is assumed that a large fraction of WSOC is formed from oxidation reactions of volatile organic compounds, although it can also come from biomass burning (López-Caravaca et al., 2023; Pio et al., 2007; Suto and Kawashima, 2021; Xie et al., 2016). In order to provide a first insight into the origin of WSOC in the study area, WSOC was correlated against oxalate (which can be considered as a marker of secondary organic aerosols; Petit et al., 2019), as well as with levoglucosan and potassium, used as tracers of biomass burning (Bhattarai et al., 2019; Suto and Kawashima, 2021). The correlation coefficients, all statistically significant at the 95% confidence level, were 0.75, 0.49 and 0.85 with oxalate, levoglucosan and K^+, respectively. These findings suggest that WSOC in the study area was the result of secondary aerosol formation and biomass burning emissions. Previous works have also reported moderate to strong correlations between WSOC and the species mentioned above (Suto and Kawashima, 2021; Theodosi et al., 2018; Zhang et al., 2012). A statistically significant correlation between WSOC and EC was also observed (r = 0.73), which could be the result of EC originating from biomass combustion, although a certain contribution from traffic emissions cannot be completely ruled out (López-Caravaca et al., 2023; Xie et al., 2016). In contrast, no correlations between water-insoluble organic carbon (WIOC), calculated by subtracting WSOC from OC, and biomass burning markers was observed, indicating that insoluble organic components must come from other sources. A limited contribution from biomass burning to WIOC concentrations have also been found in previous studies (Sciare et al., 2011) since most of the organic matter emitted from wood burning is water-soluble (Dusek et al., 2017; Sciare et al., 2011). Unexpectedly, WIOC did not correlate either with EC, although fossil fuel combustion has been identified as a main source of WIOC, as indicated by its strong relationship with traffic tracers (not only EC but also carbon monoxide) in urban environments (Henningan et al., 2009; Miyazaki et al., 2006). Since wood burning and fossil fuel combustion are not likely sources of water-insoluble organic compounds at the measurements site, we hypothesise that WIOC during the sampling period was mainly due to primary biogenic emissions such as resuspended soil (Hasheminassab et al., 2014).

3.3.3. Methanol-soluble organic carbon

As expected, MSOC concentrations were significantly higher than WSOC concentrations, since methanol dissolves a larger fraction of organic compounds than water (Rathod et al., 2024). During the study period, MSOC contributed 63% to the total OC average concentration. This percentage can be considered quite low, as many studies performed both in rural and urban areas have reported values generally larger than 85% (Cheng et al., 2016; Xie et al., 2016, 2019; Zou et al., 2022).

MSOC is mainly released into the atmosphere by biomass burning (Zhang et al., 2020), although vehicle emissions and secondary organic aerosols formed from anthropogenic and biogenic precursors have been also been identified as sources of methanol-soluble organic compounds (Cao et al., 2021; Cheng et al., 2016; Xie et al., 2019; Zhang et al., 2020). Moderate correlation coefficients of MSOC with EC and soluble potassium were found in the present study ($r = 0.52$, $p < 0.05$), while no correlation with levoglucosan was observed. On the other hand, MSOC also showed a moderate positive correlation with oxalate ($r = 0.54$, $p < 0.05$). These results suggest that the variability in MSOC concentrations during the sampling campaign was not dominated by a single source. WSOC and MSOC concentrations exhibited a relatively good correlation ($r = 0.67$, $p < 0.05$), which indicates that they share some common sources. This was not unexpected since both fractions contain highly polar compounds (Cao et al., 2021).

Daily average levoglucosan concentrations ranged from 17 ng m^{-3} to 119 ng m^{-3}, and were higher at the beginning of the campaign due to lower ambient temperatures (Fig. 3). The average concentration during the whole study period was lower than the value of 68 ng m^{-3} registered in the city centre of Elche during winter (from December to February; Clemente et al., 2024). Levoglucosan levels measured at other rural locations in Europe significantly vary with sampling location. For instance, Ytti et al. (2019) reported values ranging from 12 ng m^{-3} to 668 ng m^{-3} during the winter/spring period at different rural background sites in Europe, while Maenhaut et al. (2012) found concentrations between 34 ng m^{-3} and 200 ng m^{-3} (median values) during winter at rural stations in Flanders (Belgium). Based on these results, moderate contributions from biomass burning to PM_{10} at our sampling location compared to other European rural sites can be expected.

3.4. Metals

Average concentrations of major and trace metals, excluding the first two days of the sampling period, are shown in Table 3. Mean concentrations for these two days affected by African dust (AD) are also shown in order to illustrate the huge influence of these events on the levels of crustal elements, as already observed at a high mountain site located in the same study region (Galindo et al., 2017). It is important to mention that calcium in the study area is in the form of soluble salts, such as $CaCO_3$ and $Ca(NO_3)_2$, as demonstrated by the strong correlation between Ca concentrations measured by ion chromatography and ED-XRF (slope = 1.06, $r = 0.94$, $p < 0.05$). Because Mn, V and Cu had concentrations below the detection limit in a significant number of samples (between 10% and 35%), gaps were filled with half the detection limit.

Strong correlations among K, Ca, Fe, Ti and V were found ($r = 0.64–0.94$, $p < 0.05$), indicating a common crustal origin. Although the correlation coefficients of these metals with Mn were generally lower ($r = 0.41–0.72$), they were statistically significant ($p < 0.05$), suggesting that Mn mainly comes from soil dust. Zn was positively correlated with EC ($r = 0.61$, $p < 0.05$), which points to traffic as the main source of zinc.

The levels of all metals were considerably lower than those previously measured at the traffic site in the city of Elche, particularly for Fe, Mn, V, Cu and Zn (annual mean levels for these metals in Elche were 399, 14, 7, 16, and 26 ng m^{-3}, respectively; Galindo et al., 2018). These results indicate a significant contribution from road traffic to the levels of the mentioned species in urban areas. It is well known that brake abrasion is an important source of Fe (also emitted from road surface wear), Cu and Mn, while tyre wear is considered as the main contributor to atmospheric Zn (Piscitello et al., 2021). Zn concentrations obtained in the present work were also low compared to other rural sites in central

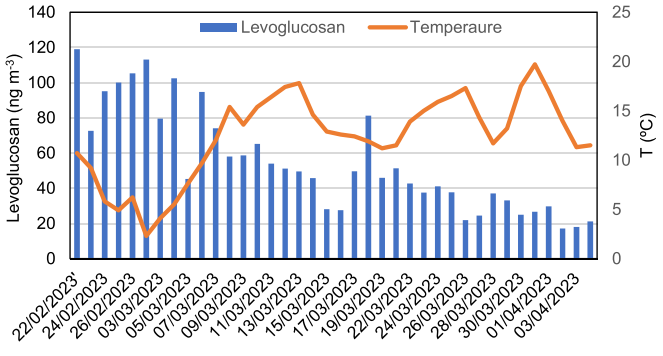

Fig. 3. Daily temperatures and levoglucosan concentrations during the study period.

Table 3
Mean concentrations and standard deviations (SD) of the metals analysed in PM_{10}, excluding the two days of high Saharan dust loadings. Average concentrations for these two days are also shown (AD). All concentrations are given in ng m^{-3}.

Metal	Mean	SD	AD
K	176	63	937
Ca	898	398	1689
Fe	128	55	1546
Ti	15	7	198
Mn	5	2	43
V	2	1	26
Cu	3	2	2
Zn	9	3	17

(15 ng m^{-3}; summer average; Mach et al., 2021) and southern Europe (21 ng m^{-3}, winter average; Pietrogrande et al., 2021).

3.5. Association of oxidative potential with PM_{10} chemical components

Table 4 presents a statistical summary of volume normalised and mass normalised OP values performed by the AA and DTT assays during the study period. OP^{AA} levels measured at the traffic site in Elche (Clemente et al., 2023a) during winter (0.71 nmol min^{-1} m^{-3} and 0.029 nmol min^{-1} μg^{-1}) were considerably higher than those found in the present study. The same rural-urban gradient has been observed in previous works (Borlaza et al., 2022; Grange et al., 2022, in 't Veld et al., 2023; Vörösmarty et al., 2023), which may be an indication that the composition of particles in rural areas makes them less oxidant than in urban environments. Conversely, for the DTT method, differences were not as well-defined and winter OP values at the urban site (0.40 nmol min^{-1} m^{-3} and 0.018 nmol min^{-1} μg^{-1}; Clemente et al., 2023a) were similar to those measured at the rural station, especially mass normalised values, although PM_{10} concentrations were around 20% higher at the urban site (24.2 μg m^{-3}, Clemente et al., 2023a). This implies that the intrinsic OP^{DTT} is the same at both locations. Shaffer et al. (2006) also observed a limited variability in the DTT activity of PM samples collected at urban canyon, urban background and rural sites in Europe. Likewise, they found that variations across sites were lower for mass-normalised than for volume-normalised values. These outcomes suggest that chemical drivers of DTT activity are similar between sites and that some of these drivers are regional and not dominated, for example, by fresh vehicle emissions (Shafer et al., 2016 and references cited therein).

The most likely reason for the differences in the spatial behaviour of OP^{DTT} and OP^{AA} is that both assays are sensitive to different PM components, as pointed out in many previous works (Bates et al., 2019; Borlaza et al., 2022; Clemente et al., 2023a; Grange et al., 2022). The linear correlation analysis between volume normalised DTT and AA activities showed that the two datasets were moderately correlated ($r = 0.52$, $p < 0.05$). The slope of the regression line between OP^{DTT} and OP^{AA} normalised by volume was lower than unity (0.68 ± 0.19), suggesting that the OP^{AA} is more sensitive to changes in PM chemical composition than the OP^{DTT} (Vörösmarty et al., 2023). This can contribute to explain the higher variability in the OP measured by the AA assay compared to the DTT method as a function of the site typology (rural-urban). The above findings are in agreement with the outcomes of Calas et al. (2019), who found larger inter-site variations in the OP^{AA} than in the OP^{DTT} between different urban areas in France.

Table 4
Average, standard deviations (SD), maximum, and minimum OP levels at the rural station of Benejama. OP_v is expressed in nmol min^{-1} m^{-3}, while and OP_m is given in nmol min^{-1} μg^{-1}.

OP	Mean	SD	Max	Min
OP_v^{AA}	0.11	0.06	0.27	0.03
OP_v^{DTT}	0.32	0.09	0.59	0.21
OP_m^{AA}	0.006	0.003	0.016	0.002
OP_m^{DTT}	0.018	0.008	0.040	0.008

In order to contextualize our observations, OP values were compared with those from recent studies performed at rural stations in Europe (Table 5). However, it is important to bear in mind that comparisons are hampered by differences in the analytical protocols (such as the initial concentration of AA and DTT or the concentration of PM added to the assay), the season of the sampling campaign and the size fraction of particles. Regarding the use of different analytical procedures, previous studies have reported a non-linear dependency between OP values and PM mass concentrations, especially in samples with significant contributions of soluble transition metals such as Cu and Mn (Charrier et al., 2016; Shahpoury et al., 2022).

OP values measured in the present work were low compared with those found in other European rural areas, in particular for the AA assay. From the data shown in Table 5 it can be inferred that there is not a direct relationship between OP levels and PM concentrations, as suggested in other works (Clemente et al., 2023a; Calas et al., 2019).

Pearson's correlation analysis was used to evaluate the association between OP values and specific PM_{10} components (Table 6). The correlation coefficients with PM_{10} concentrations are also shown. In order to avoid the effect of extreme concentrations of some species on the results of the correlation study, the two days under the influence of high Saharan dust loadings were excluded from the analysis.

As already observed at the traffic site located in Elche (Clemente et al., 2023a), the DTT activity was better correlated with a wide variety of chemical species than the AA activity. These outcomes differ from those obtained by Pietrogrande et al. (2021), who found similar associations between both assays and PM_{10} components at the rural site of Novaledo (Italy). Our findings suggest that, during the study period, there was not a clear source associated with the OP^{AA} at the rural station. Instead, the variability in the daily AA activity was affected by different sources, as suggested by the marginal correlations with traffic tracers (EC and Zn) and secondary ions (nitrate, sulfate and oxalate). It is important to mention that water-soluble ions are not redox-active; therefore, their correlation with the AA assay may indicate a certain contribution of secondary aerosol formation to the OP^{AA}. Although a statistically significant correlation with K^+ was observed, OP^{AA} values were not correlated with levoglucosan, which suggests that biomass burning emissions did not significantly contribute to OP^{AA} levels during the measurement period.

The OP^{DTT} showed the best correlations with WSOC and soluble potassium, which points to biomass burning as an important driver of the DTT activity during the measurement period. This result is in agreements with previous studies, which found that wood burning is a significant source for OP^{DTT} during the cold period (Bates et al., 2019; Calas et al., 2018). Strong correlations between DTT measurements and WSOC has been reported in a number of previous works, indicating that water-soluble organic matter, such as quinones and humic-like compounds, is the main material associated with DTT consumption (Bates et al., 2019; Pietrogrande et al., 2021; Verma et al., 2015; Wang et al., 2020).

Differently from the results of other works performed in rural areas (in 't Veld et al., 2023 Pietrogrande et al., 2021), no correlation between OP values and PM_{10} concentrations were found in the present study, which indicates that the temporal variability of both parameters is driven by different sources. A possible reason for this finding may be the lower contribution from anthropogenic sources (such as traffic and biomass burning), which are associated with high oxidative potential (Daellenbach et al., 2020), to PM_{10} levels at the sampling site.

4. Conclusions

The composition of PM_{10} at a rural site in southeastern Spain was dominated by organic matter (OM), although its contribution (28%) was

Table 5
OP (nmol min^{-1} m^{-3}) and PM levels (μg m^{-3}) measured at rural sites in Europe.

PM	Site	Study period	OP_v^{AA}	OP_v^{DTT}	PM concent.	Reference
PM_{10}	Benejama (southeastern Spain)	Late winter-early spring	0.11	0.32	20	This study
PM_{10}	Montsey (northeastern Spain)	Annual	0.4	0.5	~8	in 't Veld et al., 2023
PM_{10}	Magadino-Cadenazzo (Switzerland)	Annual	1.7	1.0	–	Grange et al. (2022)
PM_{10}	Payerne (Switzerland)	Annual	0.7	0.8	–	Grange et al. (2022)
PM_{10}	Novaledo (Northern Italy)	Winter	0.28	0.33	31	Pietrogrande et al. (2021)
PM_{10}	OPE (northeastern France)[a]	9 years	~0.3	~0.6	9	Borlaza et al. (2022)
$PM_{2.5}$	K-puszta (Hungary)[b]	Annual	1.5	1.2	14	Vörösmarty et al. (2023)

[a] Observatoire Pérenne de l'Environnement.
[b] Median values.

Table 6
Pearson's correlation coefficients between volume normalised OP measurements and PM_{10} chemical components. *Correlations statistically significant ($p < 0.05$). N = 36.

	OP^{AA}	OP^{DTT}
PM_{10}	0.17	0.06
Cl^-	0.04	−0.27
NO_3^-	0.57*	0.51*
SO_4^{2-}	0.34*	0.60*
CO_3^{2-}	0.04	−0.34
$C_2O_4^{2-}$	0.52*	0.67*
Na^+	0.19	−0.16
NH_4^+	0.25	0.63*
K^+	0.44*	0.73*
Mg^{2+}	0.15	0.18
Ca^{2+}	0.16	0.14
EC	0.52*	0.43*
OC	0.29	0.41*
MSOC	0.27	0.58*
WSOC	0.52*	0.81*
Levoglucosan	0.13	0.44*
K	0.00	0.13
Fe	0.14	0.03
Ti	0.08	0.02
Mn	0.13	0.08
V	0.15	0.02
Cu	0.16	0.47*
Zn	0.55*	0.53*

lower than that observed at other European rural environments probably because of the lower OM emissions from biomass burning and the higher dust loads favoured by the low plant cover. In fact, the concentrations of crustal species such as Ca^{2+} and inorganic carbon (carbonate and/or bicarbonate) were significantly higher than the values reported for other rural sites in southern Europe, due to the dominance of calcium carbonate in the soils of the study area. Water-soluble organic carbon (WSOC) and methanol-soluble organic carbon (MSOC) contributed 42% and 63% to the average OC mass concentration. These percentages are low compared with most values reported in the literature, especially for MSOC, implying that a significant fraction of the OC in the study area comprises low-solubility compounds. Pearson's correlation analyses suggest that the variability in WSOC and MSOC concentrations was influenced by emissions from biomass burning, as well as secondary aerosol formation processes.

AA activities were significantly lower than those found at an urban site within the same geographical area, while DTT activities were more similar at both locations, most likely because the redox activity of both compounds is driven by different PM components/sources. These results indicate a higher variability of the OP^{AA} as a function of the site typology although the reasons are still unclear and need additional investigation. OP^{DTT} was best correlated with WSOC and K^+ ($r > 0.7$) and showed a moderate statistically significant correlation with levoglucosan ($r = 0.44$), pointing to biomass burning as an important source for OP^{DTT}. In contrast, OP^{AA} was moderately correlated ($r < 0.57$) with secondary ions (NO_3^- and $C_2O_4^{2-}$) and traffic tracers such as EC and Zn, suggesting that there was not a single and clear source for OP^{AA} during the study period. None of the assays was correlated with PM_{10} levels, most likely because the variability of OP and PM_{10} levels is driven by different sources. This result reveals that the PM_{10} mass concentration is not always a good parameter for assessing aerosol toxicity, since it strongly depends on the sources and specific characteristics of the sampling site. On the other hand, the fact that both OP methods provide different results point to the need for further research to find a single metric suitable for aerosol toxicity measurements.

CRediT authorship contribution statement

Noelia Gómez-Sánchez: Writing – review & editing, Visualization, Investigation. **Nuria Galindo:** Writing – original draft, Supervision, Project administration, Investigation, Funding acquisition, Conceptualization. **Marina Alfosea-Simón:** Writing – review & editing, Visualization, Investigation. **Jose F. Nicolás:** Writing – review & editing, Visualization, Formal analysis. **Javier Crespo:** Writing – review & editing, Supervision, Investigation. **Eduardo Yubero:** Writing – review & editing, Supervision, Project administration, Funding acquisition, Conceptualization.

Declaration of competing interest

The authors declare that they have no known competing financial interests or personal relationships that could have appeared to influence the work reported in this paper.

Data availability

Data will be made available on request.

Acknowledgements

This work was supported by MCIN/AEI/10.13039/501100011033 and the "European Union NextGenerationEU/PRTR" (CAMBIO project, ref. TED2021-131336B–I00) and by the Valencian Regional Government (Generalitat Valenciana, CIAICO/2021/280 research project). The authors would like to thank AVAMET for supplying meteorological data and the ACTRIS-Spain network (CGL2017-90884-REDT).

References

Bates, J.T., Fang, T., Verma, V., Zeng, L., Weber, R.J., Tolbert, P.E., Abrams, J.Y., Sarnat, S.E., Klein, M., Mulholland, J.A., Russel, A.G., 2019. Review of acellular assays of ambient particulate matter oxidative potential: methods and relationships with composition, sources, and health effects. Environ. Sci. Technol. 53, 4003–4019.
Bhattarai, H., Saikawa, E., Wan, X., Zhu, H., Ram, K., Gao, S., Kang, S., Zhang, Q., Zhang, Y., Wu, G., Wang, X., Kawamura, K., Fu, P., Cong, Z., 2019. Levoglucosan as a tracer of biomass burning: recent progress and perspectives. Atmos. Res. 220, 20–33.
Błaszczak, B., Mathews, B., 2020. Characteristics of carbonaceous matter in aerosol from selected urban and rural areas of Southern Poland. Atmosphere 11, 687.
Borlaza, L.J., Weber, S., Marsal, A., Uzu, G., Jacob, V., Besombes, J.L., Chatain, M., Conil, S., Jaffrezo, J.L., 2022. Nine-year trends of PM_{10} sources and oxidative potential in a rural background site in France. Atmos. Chem. Phys. 22, 8701–8723.

Borroni, E., Pesatori, A.C., Bollati, V., Buoli, M., Carugno, M., 2022. Air pollution exposure and depression: a comprehensive updated systematic review and meta-analysis. Environ. Pollut. 292, 118245.
Calas, A., Uzu, G., Kelly, F.J., Houdier, S., Martins, J.M.F., Thomas, F., Molton, F., Charron, A., Dunster, C., Oliete, A., Jacob, V., Besombes, J.-L., Chevrier, F., Jaffrezo, J.-L., 2018. Comparison between five acellular oxidative potential measurement assays performed with detailed chemistry on PM_{10} samples from the city of Chamonix (France). Atmos. Chem. Phys. 18, 7863–7875.
Calas, A., Uzu, G., Besombes, J.-L., Martins, J.M.F., Redaelli, M., Weber, S., Charron, A., Albinet, A., Chevrier, F., Brulfert, G., Mesbah, B., Favez, O., Jaffrezo, J.-L., 2019. Seasonal variations and chemical predictors of oxidative potential (OP) of particulate matter (PM), for seven urban French sites. Atmosphere 10, 698.
Cao, T., Li, M., Zou, C., Fan, X., Song, J., Jia, W., Yu, C., Yu, Z., Peng, P., 2021. Chemical composition, optical properties, and oxidative potential of water- and methanol-soluble organic compounds emitted from the combustion of biomass materials and coal. Atmos. Chem. Phys. 21, 13187–13205.
Charrier, J.G., McFall, A.S., Vu, K.K.T., Baroi, J., Olea, C., Hasson, A., Anastasio, C., 2016. A bias in the "mass-normalized" DTT response – an effect of non-linear concentration-response curves for copper and manganese. Atmos. Environ. 144, 325–334.
Cheng, Y., He, K., Du, Z., Engling, G., Liu, J., Ma, Y., Zheng, M., Weber, R.J., 2016. The characteristics of brown carbon aerosol during winter in Beijing. Atmos. Environ. 127, 355–364.
Chiari, M., Yubero, E., Calzolai, G., Lucarelli, F., Crespo, J., Galindo, N., Nicolás, J.F., Giannoni, M., Nava, S., 2018. Comparison of PIXE and XRF analysis of airborne particulate matter samples collected on Teflon and quartz fibre filters. Nucl. Instrum. Methods B 417, 128–132.
Chirino, Y.I., Sánchez-Pérez, Y., Osornio-Vargas, A.R., Morales-Bárcenas, R., Gutiérrez-Ruiz, M.C., Segura-García, Y., Rosas, I., Pedraza-Chaverri, J., García-Cuéllar, C.M., 2010. PM_{10} impairs the antioxidant defense system and exacerbates oxidative stress driven cell death. Toxicol. Lett. 193, 209–216.
Chow, J.C., Lowenthal, D.H., Chen, L.W.A., Wang, X., Watson, J.G., 2015. Mass reconstruction methods for $PM_{2.5}$: a review. Air Qual. Atmos. Health. 8, 243–263.
Clemente, Á., Gil-Moltó, J., Yubero, E., Juárez, N., Nicolás, J.F., Crespo, J., Galindo, N., 2023a. Sensitivity of PM_{10} oxidative potential to aerosol chemical composition at a Mediterranean urban site: ascorbic acid versus dithiothreitol measurements. Air Qual. Atmos. Health 16, 1165–1172.
Clemente, Á., Galindo, N., Nicolás, J.F., Crespo, J., Pastor, C., Yubero, E., 2023b. Local versus regional contributions to PM_{10} levels in the Western Mediterranean. Aerosol Air Qual. Res. 23, 230218.
Clemente, Á., Yubero, E., Nicolás, J.F., Crespo, J., Galindo, N., 2024. Organic tracers in fine and coarse aerosols at an urban Mediterranean site: contribution of biomass burning and biogenic emissions. Environ. Sci. Pollut. Res. (in press).
Dinoi, A., Cesari, D., Marinoni, A., Bonasoni, P., Riccio, A., Chianese, E., Tirimberio, G., Naccarato, A., Sprovieri, F., Andreoli, V., et al., 2017. Inter-Comparison of carbon content in $PM_{2.5}$ and PM_{10} collected at five measurement sites in Southern Italy. Atmosphere 8, 243.
Daellenbach, K.R., Uzu, G., Jiang, J., Cassagnes, L.E., Leni, Z., Vlachou, A., Stefenelli, G., Canonaco, F., Weber, S., Segers, A., et al., 2020. Sources of particulate-matter air pollution and its oxidative potential in Europe. Nature 587, 414–419.
Dominutti, P.A., Borlaza, L.J.S., Sauvain, J.J., Thuy, V.D.N., Houdier, S., Suarez, G., Jaffrezo, J.L., Tobin, S., Trébuchon, C., Socquet, S., et al., 2023. Source apportionment of oxidative potential depends on the choice of the assay: insights into 5 protocols comparison and implications for mitigation measures. Environ. Sci.: Atmos. 3, 1497–1512.
Dusek, U., Hitzenberger, R., Kasper-Giebl, A., Kistler, M., Meijer, H.A.J., Szidat, S., Wacker, L., Holzinger, R., Röckmann, T., 2017. Sources and formation mechanisms of carbonaceous aerosol at a regional background site in The Netherlands: insights from a year-long radiocarbon study. Atmos. Chem. Phys. 17, 3233–3251.
EEA, 2022. Air Quality in Europe – 2022 Report. European Environment Agency. https://doi.org/10.2800/488115. EEA Report No. 05/2022.
Galindo, N., Yubero, E., 2017. Day-night variability of water-soluble ions in PM_{10} samples collected at a traffic site in southeastern Spain. Environ. Sci. Pollut. Res. 24, 805–812.
Galindo, N., Yubero, E., Nicolás, J.F., Crespo, J., Varea, M., Gil-Moltó, J., 2017. Regional and long-range transport of aerosols at Mt. Aitana, Southeastern Spain. Sci. Total Environ. 584–585, 723–730.
Galindo, N., Yubero, E., Nicolás, J.F., Varea, M., Crespo, J., 2018. Characterization of metals in PM_1 and PM_{10} and health risk evaluation at an urban site in the western Mediterranean. Chemosphere 201, 243–250.
Galindo, N., Clemente, Á., Yubero, E., Nicolás, J.F., Crespo, J., 2021. PM_{10} chemical composition at a residential site in the western Mediterranean: estimation of the contribution of biomass burning from levoglucosan and its isomers. Environ. Res. 196, 110394.
Grahame, T.J., Schlesinger, R.B., 2012. Oxidative stress-induced telomeric erosion as a mechanism underlying airborne particulate matter-related cardiovascular disease. Part. Fibre Toxicol. 9, 21.
Grange, S.K., Uzu, G., Weber, S., Jafrezzo, J.L., Hueglin, C., 2022. Linking Switzerland's PM_{10} and $PM_{2.5}$ oxidative potential (OP) with emission sources. Atmos. Chem. Phys. 22, 7029–7050.
Hannam, K., McNamee, R., Baker, P., Sibley, C., Agius, R., 2014. Air pollution exposure and adverse pregnancy outcomes in a large UK birth cohort: use of a novel spatio-temporal modelling technique. Scand. J. Work. Environ. Health 40, 518–530.
Hasheminassab, S., Daher, N., Shafer, M.M., Schauer, J.J., Delfino, R.J., Sioutas, C., 2014. Chemical characterization and source apportionment of indoor and outdoor fine particulate matter ($PM_{2.5}$) in retirement communities of the Los Angeles Basin. Sci. Total Environ. 490, 528–537.
Henningan, C.J., Bergin, M.H., Russel, A.G., Nenes, A., Weber, R.J., 2009. Gas/particle partitioning of water-soluble organic aerosol in Atlanta. Atmos. Chem. Phys. 9, 3613–3628.
in 't Veld, M., Pandolfi, M., Amato, F., Pérez, N., Reche, C., Dominutti, P., Jafrezzo, J., Alastuey, A., Querol, X., Uzu, G., 2023. Discovering oxidative potential (OP) drivers of atmospheric PM_{10}, $PM_{2.5}$, and PM_1 simultaneously in North-Eastern Spain. Sci. Total Environ. 857, 159386.
Jiang, Y., Zhuang, G., Wang, Q., Liu, T., Huang, K., Fu, J.S., Li, J., Lin, Y., Zhang, R., Deng, C., 2014. Aerosol oxalate and its implication to haze pollution in Shanghai, China. Chin. Sci. Bull. 59, 227–238.
Kilian, J., Kitazawa, M., 2018. The emerging risk of exposure to air pollution on cognitive decline and Alzheimer's disease - evidence from epidemiological and animal studies. Biomed. J. 41, 141–162.
Laongsri, B., Harrison, R.M., 2013. Atmospheric behaviour of particulate oxalate at UK urban background and rural sites. Atmos. Environ. 71, 319–326.
Li, X., Yu, F., Song, Y., Zhang, C., Yan, F., Hu, Z., Lei, Y., Tripathee, L., Zhang, R., Wang, Y., et al., 2023. Water-soluble brown carbon in PM2.5 at two typical sites in Guanzhong Basin: optical properties, sources, and implications. Atmos. Res. 281, 106499.
Lionetto, M.G., Guascito, M.R., Giordano, M.E., Caricato, R., De Bartolomeo, A.R., Romano, M.P., Conte, M., Dinoi, A., Contini, D., 2021. Oxidative potential, cytotoxicity, and intracellular oxidative stress generating capacity of PM_{10}: a case study in south of Italy. Atmosphere 12, 464.
López-Caravaca, A., Crespo, J., Galindo, N., Yubero, E., Juárez, N., Nicolás, J.F., 2023. Sources of water-soluble organic carbon in fine particles at a southern European urban background site. Atmos. Environ. 306, 119844.
Mach, T., Rogula-Kozłowska, W., Bralewska, K., Majewski, G., Rogula-Kopiec, P., Rybak, J., 2021. Impact of municipal, road traffic, and natural sources on PM_{10}: the hourly variability at a rural site in Poland. Energies 14, 2654.
Maenhaut, W., Vermeylen, R., Claeys, M., Vercauteren, J., Matheeussen, C., Roekens, E., 2012. Assessment of the contribution from wood burning to the PM_{10} aerosol in Flanders, Belgium. Sci. Total Environ. 437, 226–236.
Malaguti, A., Mircea, M., La Torretta, T.M., Telloli, C., Petralia, E., Stracquadanio, M., Berico, M., 2015. Chemical composition of fine and coarse aerosol particles in the Central Mediterranean area during dust and non-dust conditions. Aerosol Air Qual. Res. 15, 410–425.
Millero, F.J., Feistel, R., Wright, D.G., McDougall, T.J., 2008. The composition of standard seawater and the definition of the reference-composition salinity scale. Deep-Sea Res. II: Top. Stud. Oceanogr. 55, 50–72.
Miyazaki, Y., Kondo, Y., Takegawa, N., Komazaki, Y., Fukuda, M., Kawamura, K., Mochida, M., Okuzawa, K., Weber, R.J., 2006. Time-resolved measurements of water-soluble organic carbon in Tokyo. J. Geophys. Res. Atmos. 111, D23206.
Navarro-Selma, B., Clemente, A., Nicolás, J.F., Crespo, J., Carratalá, A., Lucarelli, F., Giardi, F., Galindo, N., Yubero, E., 2022. Size segregated ionic species collected in a harbour area. Chemosphere 294, 133693.
Newell, K., Kartsonaki, C., Lam, K.B.H., Kurmi, O.P., 2017. Cardiorespiratory health effects of particulate ambient air pollution exposure in low-income and middle-income countries: a systematic review and meta-analysis. Lancet Planet. Health 1, e368–e380.
Nicolás, J.F., Galindo, N., Yubero, E., Pastor, C., Esclapez, R., Crespo, J., 2009. Aerosol inorganic ions in a semiarid región on the southeastern Spanish Mediterranean coast. Water Air Soil Pollut. 201, 149–159.
Pachon, J.E., Weber, R.J., Zhang, X., Mulholland, J.A., Russell, A.G., 2013. Revising the use of potassium (K) in the source apportionment of $PM_{2.5}$. Atmos. Pollut. Res. 4, 14–21.
Patel, A., Rastogi, N., 2018. Seasonal variability in chemical composition and oxidative potential of ambient aerosol over a high altitude site in western India. Sci. Total Environ. 644, 1268–1276.
Pérez-Pastor, R., Salvador, P., García-Alonso, S., Alastuey, A., García dos Santos, S., Querol, X., Artíñano, B., 2020. Characterization of organic aerosol at a rural site influenced by olive waste biomass burning. Chemosphere 248, 125896.
Petit, J.-E., Pallarès, C., Favez, O., Alleman, L.Y., Bonnaire, N., Rivière, E., 2019. Sources and geographical origins of PM_{10} in Metz (France) using oxalate as a marker of secondary organic aerosols by positive matrix factorization analysis. Atmosphere 10, 370.
Pietrogrande, M.C., Russo, M., Zagatti, E., 2019. Review of PM oxidative potential measured with acellular assays in urban and rural sites across Italy. Atmosphere 10, 626.
Pietrogrande, M.C., Bertoli, I., Clauser, G., Dalpiaz, C., Dell'Anna, R., Lazzeri, P., Lenzi, W., Russo, M., 2021. Chemical composition and oxidative potential of atmospheric particles heavily impacted by residential wood burning in the alpine region of northern Italy. Atmos. Environ. 253, 118360.
Pietrogrande, M.C., Romanato, L., Russo, M., 2022. Synergistic and antagonistic effects of aerosol components on its oxidative potential as predictor of particle toxicity. Toxics 10, 196.
Pio, C., Legrand, M., Oliveira, T., Afonso, J., Santos, C., Caseiro, A., Fialho, P., Barata, F., Puxbaum, H., Sánchez-Ochoa, A., et al., 2007. Climatology of aerosol composition (organic versus inorganic) at nonurban sites on a west-east transect across Europe. J. Geophys. Res. 112, D23S02.
Piscitello, A., Bianco, C., Casasso, A., Sethi, R., 2021. Non-exhaust traffic emissions: sources, characterization, and mitigation measures. Sci. Total Environ. 766, 144440.
Ram, K., Sarin, M.M., 2010. Spatio-temporal variability in atmospheric abundances of EC, OC and WSOC over Northern India. J. Aerosol Sci. 41, 88–98.

Rathod, T.D., Sahu, S.K., Tiwari, M., Bhangare, R.C., Ajmal, P.Y., 2024. Optical properties of water soluble and organic soluble carbonaceous aerosols at an urban location in India. Atmos. Pollut. Res. 15, 101956.
Sandrini, S., van Pinxteren, D., Giulianelli, L., Herrmann, H., Poulain, L., Facchini, M.C., Gilardoni, S., Rinaldi, M., Paglione, M., Turpin, B.J., et al., 2016. Size-resolved aerosol composition at an urban and a rural site in the Po Valley in summertime: implications for secondary aerosol formation. Atmos. Chem. Phys. 16, 10879–10897.
Scerri, M.M., Kandler, K., Weinbruch, S., 2016. Disentangling the contribution of Saharan dust and marine aerosol to PM_{10} levels in the Central Mediterranean. Atmos. Environ. 147, 395–408.
Sciare, J., d'Argouges, O., Sarda-Estève, R., Gaimoz, C., Dolgorouky, C., Bonnaire, N., Favez, O., Bonsang, B., Gros, V., 2011. Large contribution of water-insoluble secondary organic aerosols in the region of Paris (France) during wintertime. J. Geophys. Res. 116, D22203.
Shafer, M.M., Hemming, J.D.C., Antkiewicz, D.S., Schauer, J.J., 2016. Oxidative potential of size-fractionated atmospheric aerosol in urban and rural sites across Europe. Faraday Discuss 189, 381–405.
Shahpoury, P., Zhang, Z.W., Filippi, A., Hildmann, S., Lelieveld, S., Mashtakov, B., Patel, B.R., Traub, A., Umbrio, D., Wietzoreck, M., et al., 2022. Inter-comparison of oxidative potential metrics for airborne particles identifies differences between acellular chemical assays. Atmos. Pollut. Res. 13, 101596.
Suto, N., Kawashima, H., 2021. Measurement report: source characteristics of water-soluble organic carbon in $PM_{2.5}$ at two sites in Japan, as assessed by long-term observation and stable carbon isotope ratio. Atmos. Chem. Phys. 21, 11815–11828.
Szidat, S., Ruff, M., Perron, N., Wacker, L., Synal, H.A., Hallquist, M., Shannigrahi, A.S., Ytri, K.E., Dye, C., Simpson, D., 2009. Fossil and non-fossil sources of organic carbon (OC) and elemental carbon (EC) in Göteborg, Sweden. Atmos. Chem. Phys. 9, 1521–1535.
Theodosi, C., Panagiotopoulos, C., Nouara, A., Zarmpas, P., Nicolaou, P., Violaki, K., Kanakidou, M., Sempéré, R., Mihalopoulos, N., 2018. Sugars in atmospheric aerosols over the eastern mediterranean. Prog. Oceanogr. 163, 70–81.
Turner, M.C., Andersen, Z.J., Baccarelli, A., Diver, W.R., Gapstur, S.M., Pope III, C.A., Prada, D., Samet, J., Thurston, G., Cohen, A., et al., 2020. Outdoor air pollution and cancer: an overview of the current evidence and public health recommendations. CA A Cancer J. Clin. 70, 460–479.
Urban, R.C., Lima-Souza, M., Caetano-Silva, L., Queiroz, M.E.C., Nogueira, R.F.P., Allen, A.G., Cardoso, A.A., Held, G., Campos, M.L.A.M., 2012. Use of levoglucosan, potassium, and water-soluble organic carbon to characterize the origins of biomass burning aerosols. Atmos. Environ. 61, 562–569.
Verma, V., Fang, T., Xu, L., Peltier, R.E., Russell, A.G., Ng, N.L., Weber, R.J., 2015. Organic aerosols associated with the generation of reactive oxygen species (ROS) by water-soluble $PM_{2.5}$. Environ. Sci. Technol. 49, 4646–4656.
Vörösmarty, M., Uzu, G., Jafrezzo, J.L., Dominutti, P., Kertész, Z., Papp, E., Salma, I., 2023. Oxidative potential in rural, suburban and city centre atmospheric environments in central Europe. Atmos. Chem. Phys. 23, 14255–14269.
Wang, Y., Wang, M., Li, S., Sun, H., Mu, Z., Zhang, L., Li, Y., Chen, Q., 2020. Study on the oxidation potential of the water-soluble components of ambient $PM_{2.5}$ over Xi'an, China: pollution levels, source apportionment and transport pathways. Environ. Int. 136, 105515.
Xie, M., Mladenov, C., Williams, M.W., Neff, J.C., Wasswa, J., Hannigan, M.P., 2016. Water soluble organic aerosols in the Colorado Rocky Mountains, USA: composition, sources and optical properties. Sci. Rep. 6, 39339.
Xie, M., Chen, X., Holder, A.L., Hays, M.D., Lewandowski, M., Offenberg, J.H., Kleindienst, T.E., Jaoui, M., Hannigan, M.P., 2019. Light absorption of organic carbon and its sources at a southeastern U.S. location in summer. Environ. Pollut. 244, 38–46.
Ytti, K.E., Simpson, D., Bergström, R., Kiss, G., Szidat, S., Ceburnis, D., Eckhardt, S., Hueglin, C., Nøjgaard, J.K., Perrino, C., et al., 2019. The EMEP Intensive Measurement Period campaign, 2008–2009: characterizing carbonaceous aerosol at nine rural sites in Europe. Atmos. Chem. Phys. 19, 4211–4233.
Zhang, X., Liu, J., Parker, E.T., Hayes, P.L., Jimenez, J.L., Gouw, J.A., Flynn, J.H., Grossberg, N., Lefer, B.L., Weber, R.J., 2012. On the gas-particle partitioning of soluble organic aerosol in two urban atmospheres with contrasting emissions: 1. Bulk water-soluble organic carbon. J. Geophys. Res. 117, D00V16.
Zhang, Y., Albinet, A., Petit, J.E., Jacob, V., Chevrier, F., Gille, G., Pontet, S., Chrétien, E., Dominik-Sègue, M., Levigoureux, G., et al., 2020. Substantial brown carbon emissions from winter residential wood burning over France. Sci. Total Environ. 743, 140752.
Zhou, Y., Huang, X.H., Bian, Q., Griffith, S.M., Louie, P.K.K., Yu, J.Z., 2015. Sources and atmospheric processes impacting oxalate at a suburban coastal site in Hong Kong: insights inferred from 1 year hourly measurements. J. Geophys. Res. Atmos. 120, 9772–9788.
Zou, C., Wang, J., Hu, K., Li, J., Yu, C., Zhu, F., Huang, H., 2022. Distribution characteristics and source apportionment of winter carbonaceous aerosols in a rural area in Shandong, China. Atmosphere 13, 1858.